

## Near haploidization is a genomic hallmark which defines a molecular subgroup of giant cell glioblastoma

Tiffany G. Baker<sup>†</sup>, Jay Alden<sup>†</sup>, Adrian M. Dubuc<sup>†</sup>, Cynthia T. Welsh, Iya Znoyko, Linda D. Cooley, Midhat S. Farooqi, Stuart Schwartz, Yvonne Y. Li, Andrew D. Cherniack, Scott M. Lindhorst, Melissa Gener, Dayna J. Wolff, and David M. Meredith<sup>®</sup>

*Department of Pathology and Laboratory Medicine, Medical University of South Carolina, Charleston, South Carolina, USA (T.G.B., J.A., C.T.W., I.Z., M.G., D.J.W.); Department of Pathology, Brigham and Women's Hospital and Harvard Medical School, Boston, Massachusetts, USA (A.M.D., D.M.M.); Department of Pathology and Laboratory Medicine, Children's Mercy Hospital and University of Missouri-Kansas City School of Medicine, Kansas City, Missouri, USA (L.D.C., M.S.F.); Cytogenetics Laboratory, Laboratory Corporation of America® Holdings, Research Triangle Park, North Carolina, USA (S.S.); Department of Medical Oncology, Dana-Farber Cancer Institute, Boston, Massachusetts, USA (Y.Y.L., A.D.C.); Broad Institute of MIT and Harvard, Cambridge, Massachusetts, USA (Y.Y.L., A.D.C.); Department of Neurosurgery, Medical University of South Carolina, Charleston, South Carolina, USA (S.M.L.)*

**Corresponding Author:** David M. Meredith, MD, PhD, Department of Pathology, Brigham and Women's Hospital, 75 Francis Street, Boston, MA 02115, USA ([dmmeredith@bwh.harvard.edu](mailto:dmmeredith@bwh.harvard.edu)).

<sup>†</sup>These authors contributed equally to this work.

### Abstract

**Background.** Giant cell glioblastoma (gcGBM) is a rare histologic subtype of glioblastoma characterized by numerous bizarre multinucleate giant cells and increased reticulin deposition. Compared with conventional isocitrate dehydrogenase (IDH)-wildtype glioblastomas, gcGBMs typically occur in younger patients and are generally associated with an improved prognosis. Although prior studies of gcGBMs have shown enrichment of genetic events, such as *TP53* alterations, no defining aberrations have been identified. The aim of this study was to evaluate the genomic profile of gcGBMs to facilitate more accurate diagnosis and prognostication for this entity.

**Methods.** Through a multi-institutional collaborative effort, we characterized 10 gcGBMs by chromosome studies, single nucleotide polymorphism microarray analysis, and targeted next-generation sequencing. These tumors were subsequently compared to the genomic and epigenomic profile of glioblastomas described in The Cancer Genome Atlas (TCGA) dataset.

**Results.** Our analysis identified a specific pattern of genome-wide massive loss of heterozygosity (LOH) driven by near haploidization in a subset of glioblastomas with giant cell histology. We compared the genomic signature of these tumors against that of all glioblastomas in the TCGA dataset ( $n = 367$ ) and confirmed that our cohort of gcGBMs demonstrated a significantly different genomic profile. Integrated genomic and histologic review of the TCGA cohort identified 3 additional gcGBMs with a near haploid genomic profile.

**Conclusions.** Massive LOH driven by haploidization represents a defining molecular hallmark of a subtype of gcGBM. This unusual mechanism of tumorigenesis provides a diagnostic genomic hallmark to evaluate in future cases, may explain reported differences in survival, and suggests new therapeutic vulnerabilities.

### Key Points

1. A subset of giant cell glioblastomas (gcGBM) show genome-wide loss of heterozygosity.
2. This genomic signature could improve diagnosis and prognostication in gcGBM.

## Importance of the Study

Giant cell glioblastoma (gcGBM) is a rare subtype of IDH-wildtype glioblastoma with an improved prognosis relative to non-giant cell counterparts. Herein, we describe a cohort of 10 gcGBMs with a unique genomic signature of genome-wide massive loss of heterozygosity consistent with haploidization. As the

current classification of gcGBM is based entirely on histomorphology, use of this genetic profile in conjunction with histomorphologic features may aid in assuring these rare lesions are placed into appropriate diagnostic, prognostic, and therapeutic categories now and in the future.

Recent molecular advances have revolutionized taxonomic classification among tumors of the CNS as evidenced by the introduction of the integrated molecular and histopathologic diagnoses in the 2016 update of the WHO classification of CNS tumors.<sup>1</sup> This shift in diagnostic paradigm emphasizes the importance of molecular findings in the evaluation of these tumors and ensures they are placed into the most appropriate diagnostic and prognostic categories. For instance, among diffuse gliomas, the presence of an isocitrate dehydrogenase (IDH) mutation implies a much-improved prognosis over IDH-wildtype tumors with similar histologic features. Similarly, formal incorporation of 1p/19q codeletion status permits the distinction between oligodendroglioma and astrocytoma on a purely molecular basis. The term “glioblastoma,” however, remains a broader diagnostic entity for any diffuse astrocytic tumor with high-grade histopathologic features.

Giant cell glioblastoma (gcGBM) is a rare histological variant of glioblastoma comprising approximately 1% of adult cases.<sup>2-4</sup> In addition to the usual histologic features of glioblastoma (GBM) (eg, astrocytic morphology, elevated proliferative rate, endothelial proliferation, and necrosis), gcGBM features bizarre, pleomorphic, and variably multinucleated giant cells and increased reticulin content.<sup>1</sup> Like other histologic subtypes of GBM, no defining genomic features have thus far been identified. Attempts to characterize the molecular genetics of gcGBM have been challenged by rarity and use of targeted (rather than genome-wide) genomic analyses. However, in the limited work that has been published, enrichment of mutations in a small number of genes, including *TP53*, *PTEN*, *RB1*, and *ATRX*, coupled with an overall low tumor mutational burden has been noted.<sup>1,5,6</sup> One study, however, showed an association between mismatch repair deficiency and giant cell morphology in a small cohort of GBMs.<sup>7</sup> Additionally, a potential link has been made between gcGBMs and *POLE* mutations.<sup>7,8</sup> Furthermore, certain copy number variations that occur more frequently in conventional glioblastoma, such as *EGFR* amplification and *CDKN2A* homozygous deletions, are much less frequent or absent in gcGBM.<sup>1,5,6</sup> While gcGBMs have been shown to be vulnerable to DNA damage due to a higher propensity for DNA double strand breaks,<sup>9</sup> the underlying molecular mechanisms unique to gcGBM remain unknown.

Although mostly limited to case reports, existing evidence suggests unique clinical behavior and presentation in gcGBM. Radiographically, gcGBM appears less

infiltrative than conventional glioblastoma and may mimic both non-neoplastic and neoplastic entities, such as infarct, hemorrhage, and metastatic disease.<sup>10</sup> Demographically, patients with gcGBM present at a younger median age and are more likely to receive complete resection.<sup>2</sup> Notably, the majority of published studies on adult tumors indicate a more favorable prognosis in gcGBM compared to other IDH-wildtype GBMs.<sup>2-5,11</sup> In one of the larger retrospective case series examining gcGBM patients, long-term survival (greater than 5 years) occurred nearly 4 times as often as in conventional non-gcGBM.<sup>2</sup>

Herein, we describe an interinstitutional genomic analysis of a cohort of 10 gcGBMs, which display a molecular signature distinctive from IDH-wildtype GBMs, showing massive genome-wide loss of heterozygosity (LOH). Our results suggest this genomic profile may represent the genomic hallmark of a subset of these entities, providing a novel molecular signature for improved diagnostics. Furthermore, these findings provide evidence of an unusual mechanism of tumorigenesis with the potential to reveal prognostic implications and/or new therapeutic strategies.

## Materials and Methods

### Case Selection and Clinical Features

Following the identification of 2 index cases, the archives of multiple institutions (Brigham and Women's Hospital and Harvard Medical School, Children's Mercy Hospital and University of Missouri-Kansas City School of Medicine, Laboratory Corporation of America® Holdings, and the Medical University of South Carolina) were searched for newly diagnosed GBMs that demonstrated both genome-wide massive LOH and characteristic histology consistent with gcGBMs. Out of a total of 768 GBMs, 17 additional cases were identified that showed some degree of giant cell morphology; 8 of those demonstrated massive LOH as observed in the index cases. Postsurgical diagnostic workup for the purpose of routine clinical care for each case included histologic review of hematoxylin and eosin (H&E) stained slides, variable degrees of immunohistochemical profiling, and genetic characterization with some combination of chromosome analysis ( $n = 2$ ), chromosomal microarray testing ( $n = 10$ ), next-generation sequencing (NGS) ( $n = 7$ ), and O<sup>6</sup>-methylguanine-DNA methyltransferase (*MGMT*) promoter methylation studies ( $n = 6$ ).

The patient's age and sex, anatomic location of tumor, sampling modality (biopsy vs resection), treatment regimen, radiologic appearance of tumor at presentation, and status of the patient at last follow-up (alive without evidence of recurrence, alive with recurrent disease, or deceased) were recorded where available.

### Chromosomal Microarray

Formalin-fixed, paraffin-embedded (FFPE) tissue was acquired for chromosomal microarray analysis. H&E-stained slides corresponding to the FFPE tissue blocks were examined by a board-certified neuropathologist to select optimal tissue regions. The analysis was performed on multiple platforms including the Infinium CytoSNP-850K BeadChip array, ThermoFisher OncoScan™ CNV Plus, and Agilent 1x1M as previously described.<sup>12,13</sup> Copy number changes were reported relative to the inferred tumor ploidy.

### Next-Generation Sequencing

Targeted exome sequencing using a custom hybrid capture NGS assay (OncoPanel) was performed on DNA isolated from FFPE tissue as described previously<sup>13</sup> for a subset of cases or using a hotspot mutation detection panel as previously described.<sup>14</sup>

### TCGA Data

GBM copy number and LOH calls were extracted from The Tissue Cancer Genome Atlas (TCGA) for GBM (TCGA, PanCancer Atlas) dataset from <https://gdc.cancer.gov/about-data/publications/pancanatlas>. Percentage of genome-wide LOH was calculated using autosomes. DNA methylation data were obtained across a subset of samples available from the TCGA, including both IDH-mutant and IDH-wildtype tumors. Hierarchical clustering of the top 3000 differentially methylated probesets was performed using MeV software (mev.tm4.org) as previously described.<sup>15</sup>

### Statistical Analysis

Statistical Analysis was performed using Prism 8. Differences in the frequency of copy number alterations and mutations were computed using a Fisher Exact test in our cohort of gcGBMs versus all GBMs in the TCGA dataset.

This study was conducted with Institutional Review Board approval at Brigham and Women's Hospital, Boston, MA, and at Children's Mercy Hospital, Kansas City, MO.

Microarray data used in this study are accessible in the Gene Expression Omnibus (GSE157647).

## Results

### Demographic, Clinical, and Radiologic Features of gcGBM

Our cohort consisted of 10 patients, for which variable clinical information was available for 9 (9/10), included 4 (4/9) female and 5 (5/9) male patients ranging in age from 9 to 68 years. All tumors were located in the cerebral hemispheres, and 7 (7/9) tumors were located in the frontal lobe with 2 (2/9) located in the temporal lobe. Most patients (8/9) had solitary lesions. Most cases (7/9) showed well circumscribed, contrast-enhancing lesions (Figure 1A) prompting radiologic differential diagnoses that predominantly included metastatic disease and high-grade glial neoplasms. One patient possessed a germline *TP53* mutation consistent with Li-Fraumeni syndrome. *MGMT* analysis was performed for 6 cases, 3 (3/6) of which demonstrated methylated promoter regions.

The clinical features of the cohort are summarized in Table 1.

### Pathologic Features

Slides were available for review for 9 (9/10) cases, all of which displayed typical histopathologic features of gcGBM (Table 2; Figure 1; Supplementary Figure S1), characterized by the presence of extremely large multinucleate tumor cells distributed throughout the tumors. In one case (gcGBM8), central review of the morphology was not possible; however, the accompanying pathology report indicated predominant giant cell morphology. The giant cells identified in each case were markedly pleomorphic and contained variable numbers of nuclei with prominent nucleoli, frequent nuclear pseudo-inclusions, and voluminous eosinophilic cytoplasm (Figure 1B; Supplementary Figure S1). Interspersed mononuclear tumor cells showed typical high-grade astrocytic appearance, frequently exhibiting epithelioid (9/9 cases) or spindled (4/9 cases) morphology reminiscent of gliosarcoma (not shown). Vascular proliferation and necrosis were ubiquitous. Large regions of geographic, infarct-type necrosis were common in larger samples (5/9 cases; Figure 1E; Supplementary Figure S1B,F,J,L). The mitotic activity was moderate, ranging from 5 to 18 per high power field, often with atypical mitotic forms. The Ki-67 index ranged from 21 to 60 percent. Of note, eosinophilic granular bodies were identified in 3/9 cases (Figure 1F); however, no Rosenthal fibers were observed. Of those tumors with surrounding normal brain tissue, 3/5 demonstrated sharp demarcation with minimal infiltration (Figure 1C; Supplementary Figure S1D,G). Robust perivascular and intratumoral lymphocytic inflammation was also a common feature, noted in all 9 cases (Figure 1D, Supplementary Figure S1). Immunohistochemistry for glial markers, such as GFAP, was uniformly positive.

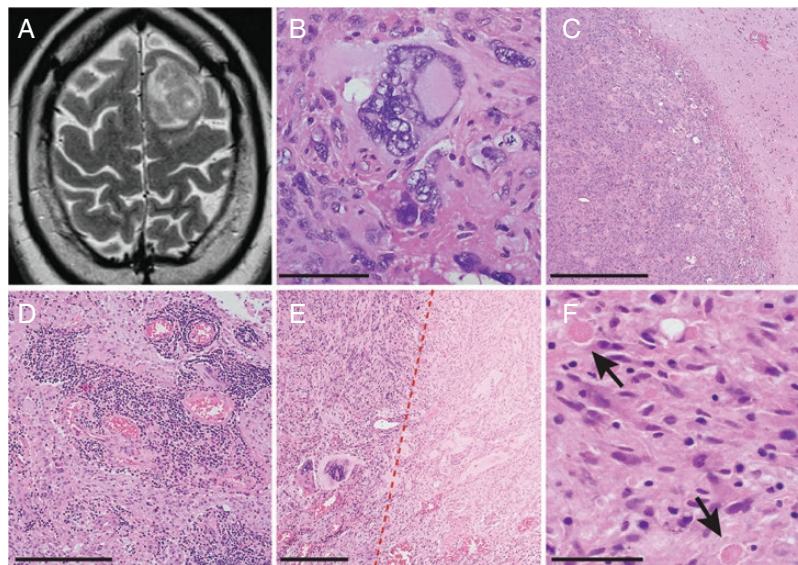


**Figure 1.** Giant cell glioblastoma (gcGBM) demonstrates specific radiographic and histological features. (A) T2-weighted MRI of gcGBM in left frontal lobe demonstrating the circumscribed nature of the tumor. (B) H&E-stained tissue section of gcGBM demonstrating the high degree of tumor cell pleomorphism, along with the presence of giant and/or multinucleated tumor cells. (C) At lower magnification, many tumors are remarkably nodular and do not exhibit diffuse infiltration into adjacent normal brain tissue. (D) Dense perivascular and intratumoral lymphocytic inflammation is common in gcGBM. (E) Many tumors showed large regions of coagulative necrosis (dotted line indicates boundary between viable tumor on the left and infarcted tumor on the right). (F) Occasional tumors contained focal eosinophilic granular bodies (arrows). Scale bars = 25  $\mu$ m in B and F, 50  $\mu$ m in D and E, 100  $\mu$ m in C.

### gcGBMs Demonstrate Consistent Genome-Wide Loss of Heterozygosity

Combinatorial use of microarray analysis and NGS revealed a remarkably consistent copy number profile with a relative gain of chromosome 7, observed in all tumors, and frequent gains of 1q and chromosome 16 (Figure 2A). No focal copy number aberrations (eg, *EGFR* amplification or homozygous *CDKN2A* deletion) were identified, and broad homozygous copy number losses were rare. Notably, allele-specific copy number profiling demonstrated a striking pattern of copy-neutral LOH affecting between 54% and 94% of the genome, with universal retention of heterozygosity of chromosome 7 (Figure 2B, Supplementary Figure S2). This observation, in the absence of a concomitant copy number loss, is most consistent with genomic near-haploidization. Chromosome studies confirmed this hypothesis by demonstrating a haploid karyotype with retention of 2 copies of chromosomes 7 in 2 tumors that were evaluated by this methodology (Figure 2C, Supplementary Figure S3). Moreover, these studies also noted frequent endoreduplication of the haploid clone leading to a near diploid state (Figure 2D).

### gcGBMs Demonstrate a Distinct Copy Number Profile From Non-gcGBMs

To evaluate the specificity of these findings, we compared the genomic profile of our tumors against a broader cohort of GBMs, both IDH-wildtype and mutated, for which

similarly comprehensive genomic data exists. To this end, we first evaluated the genome-wide copy number profile of our cohort against that of all GBMs present in the TCGA database ( $n = 367$ ). While both cohorts shared several aberrations, including copy number gain of chromosome 7, the profiles were otherwise remarkably distinct (Figure 3A). The gcGBMs in our cohort demonstrated significantly fewer copy number aberrations on average relative to other GBMs (24 vs 103,  $P < .001$ ; Figure 3B); however, these aberrations were significantly larger on average (115.2 Mb vs 36.10 Mb,  $P < .0001$ ) and generally included whole chromosome or arm level events (Figure 3C). Moreover, there was a striking absence of focal aberrations, such as *EGFR* amplifications, homozygous deletions of *CDKN2A/2B*, and relative loss of chromosome 10, which are commonly observed in GBMs. Most striking were differences in genome-wide copy-neutral LOH. While LOH (copy neutral or copy-number driven) was observed in all gcGBMs (ranging from 54% to 94% of the autosomal haploid genome; average 79%), similar levels of LOH were noted in only 1% (3/367) of GBMs in the TCGA dataset (Figure 3D, pink dots). Review of the scanned slide images of all 3 TCGA cases with massive LOH revealed clear gcGBM histology as described above.

### gcGBM Demonstrates Distinct Mutational Profile and Epigenetic Signature From Non-gcGBM

While the mutational profile of gcGBM has been previously described,<sup>1,5,6</sup> given the unexpected and unreported nature

**Table 1.** Summary of the Demographics and Clinical Parameters of the gcGBM Cohort

Tumor ID	Gender	Age (years)	MGMT Promoter Status	Resection Type	Location	Circumscribed on Imaging	Adjuvant Therapy	Status at Last Follow-up (months)
gcGBM1	Female	24	Unmethylated	Near gross total	Left frontal	Yes	RT and Optune	AWOD (18)
gcGBM2	Male	55	N/A	N/A	Right frontal	Yes	N/A	N/A
gcGBM3	Male	68	Methylated	Stereotactic biopsy	Left frontal	Yes	TMZ/RT	DOD (9)
gcGBM4	Male	57	Methylated	Near gross total	Right frontal	Yes	TMZ/RT	AWOD (8)
gcGBM5	Male	50	Methylated	Near gross total	Right frontal	No	TMZ/RT	AWD (15)
gcGBM6	Female	9	N/A	Near gross total	Right temporal	Yes	TMZ/RT	DOD (20)
gcGBM7	Female	12	N/A	Near gross total	Left frontal	Yes	TMZ/RT	DOD (41)
gcGBM8	N/A	N/A	N/A	N/A	N/A	N/A	N/A	N/A
gcGBM9	Male	57	Unmethylated	Near gross total	Right temporal	Yes	N/A	AWOD (1)
gcGBM10	Female	48	Unmethylated	Near gross total	Left frontal	Yes	TMZ/RT	DOD (14)

AWD, alive with recurrent disease; AWOD, alive without recurrent disease; DOD, died of disease; N/A, not available; RT, radiation therapy; TMZ, temozolomide.

of the copy number landscape driven by a near-haploid profile, we evaluated recurrent mutations observed in gcGBMs from our cohort (including the 3 tumors reclassified as gcGBMs from the TCGA dataset) against the remaining non-gcGBMs in the TCGA dataset. In keeping with previous reports, we observed a significantly higher frequency of mutations in *TP53* (87.5% vs 28.5%;  $P < .0011$ ) and *RB1* (75% vs 8.65%;  $P < .0001$ ; [Figure 3E](#), [Supplementary Table S1](#)). Other commonly mutated genes included *PTEN* (50%), *NF1* (30%), and *PIK3CA* (10%). Of note, no alterations were detected in *TERT* promoter region in 5 of 5 tumors for which this region was analyzed. Finally, we evaluated the epigenetic signature of gcGBMs (from TCGA tumors where this information was available) against a subset of TCGA GBMs ( $n = 17$ ), including both IDH-wildtype and IDH-mutated tumors. Hierarchical clustering only convincingly demonstrated 2 distinct subgroups, differentiating IDH-mutated from IDH-wildtype tumors. While 2 of the 3 TCGA gcGBMs cluster most closely together, the epigenetic profile was not significantly different from that observed in other IDH-wildtype GBMs ([Figure 3F](#)).

### TP53 Alterations May Drive Giant Cell Histology in the Absence of a Near-Haploid Profile

As prior studies have described variability in the degree to which giant cell features can be observed in GBMs, we performed a comprehensive evaluation of 768 GBMs and identified 9 additional cases in which the presence of giant cells were noted by histopathology report. While these tumors exhibited giant cell features, these

**Table 2.** Summary of the Histopathologic Features of the gcGBM Cohort

Features	N/Total (%)
Giant multinucleate cells	9/9 (100)
Mononuclear epithelioid cells	9/9 (100)
Spindled cells	4/9 (44)
Perivascular/intratumoral inflammation	9/9 (100)
Eosinophilic granular bodies	3/9 (33)
Nuclear pseudo-inclusions	9/9 (100)
Vascular proliferation	9/9 (100)
Necrosis	9/9 (100)
Geographic/coagulative necrosis	5/9 (56)
Atypical mitotic figures	9/9 (100)
Nodular/well-demarcated growth	3/5 (60)
Mitotic count (range) (per 10 HPF)	5–18
Ki67 index (range) (%)	21–60

HPF, High power fields.

were frequently rare or scattered, rather than the predominant pattern observed in near-haploid gcGBMs ([Supplementary Figure S4A](#)). In each of these additional cases, allele-specific copy number profile did not identify a near-haploid signature ([Supplementary Figure S4B,C](#)) but instead a copy number profile more reminiscent of IDH-wildtype GBMs, with the presence of

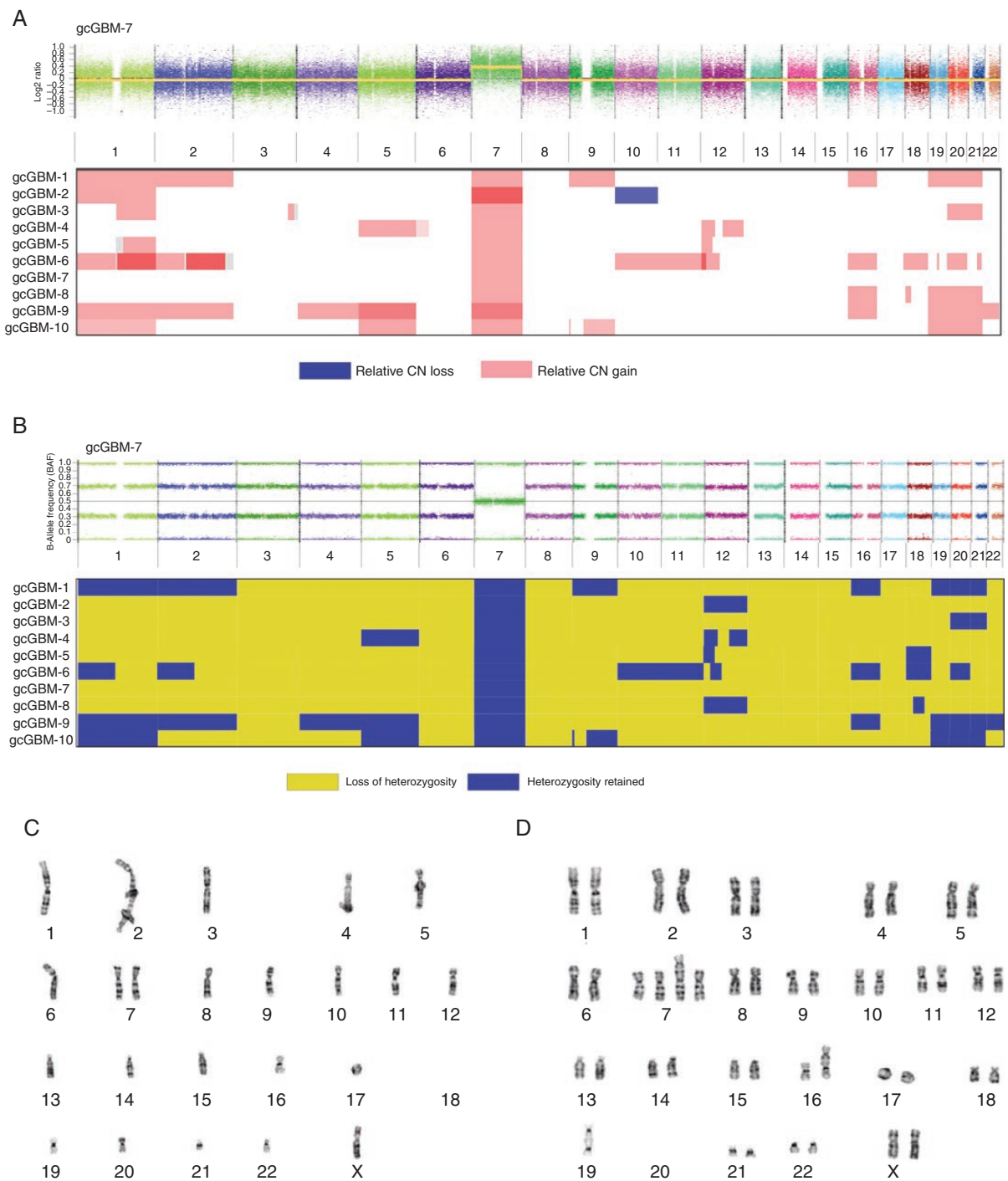


**Figure 2.** Near haploidization as a genomic hallmark of giant cell glioblastomas (gcGBMs). (A) Relative copy number landscape of gcGBMs. (B) Loss of heterozygosity (LOH) analysis of gcGBMs. (C) Stemline haploid clone identified by chromosome analysis of gcGBM7. (D) Doubled haploid clone detected in gcGBM7.

amplification events involving *EGFR* or *MDM2*, *CDKN2A* homozygous deletion, or monosomy 10. Notably, targeted molecular studies demonstrated that in 8 (8/9) of these additional cases in which TP53 sequencing was performed, an oncogenic alteration was identified (Supplementary Figure S5).

### Treatment and Outcomes

Of 8 patients with near-haploid gcGBM, sufficient available surgical history, 7 received near total resections, and one underwent biopsy, alone. Of the 7 patients with available treatment history, 6 received

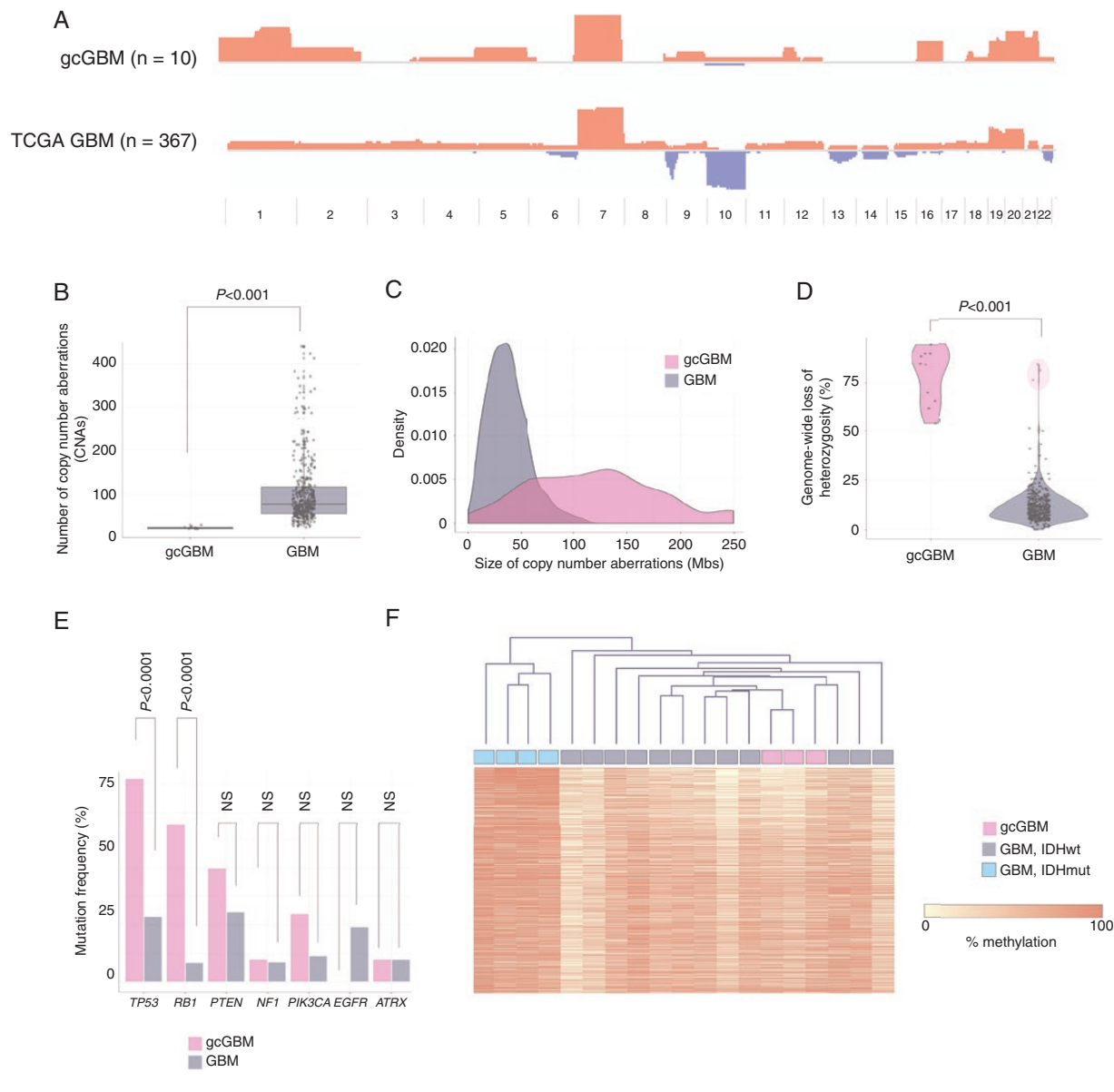


**Figure 3.** Genomic characterization of giant cell glioblastomas (gcGBMs) versus The Cancer Genome Atlas (TCGA) GBMs. (A) Summary plot of copy number analysis across gcGBM ( $n = 10$ ) cohort versus TCGA GBMs ( $n = 367$ ). (B) Frequency of copy number aberration in gcGBMs versus TCGA GBMs (C) Density plot analysis of copy number size distribution of gcGBMs versus TCGA GBMs. (D) Genome-wide loss of heterozygosity analysis. (E) Frequency of mutations observed in gcGBM cohort. (F) Hierarchical clustering analysis of gcGBMs versus isocitrate dehydrogenase (IDH)-wildtype and IDH-mutated GBMs in the TCGA cohort.

standard postoperative radiation and temozolomide chemotherapy, and 1 received only postoperative radiation therapy. Reported patient statuses at last follow-up were the following: alive without evidence of recurrence (3 patients), alive with recurrent disease (1 patient), or deceased (4 patients). Patient survival information was limited by several patients being lost to follow up but ranged from 1 to 41 months for the 8 patients where available (summarized in [Table 1](#)).

## Discussion

gcGBM is a rare subtype of IDH-wildtype GBM, with marked differences in its histological, radiographical, and clinical presentation. Histologically, these tumors are set apart by their circumscribed appearance, increased reticulin deposition, and the presence of pleomorphic and multinucleated tumor giant cells. Despite numerous

efforts to identify defining genomic, or epigenomic features, no diagnostically specific findings have been identified. These studies have, however, reported frequent inactivation of *TP53*, which was postulated by one group to be a driver event,<sup>5,6</sup> in addition to confirming their IDH-wildtype status.

Herein, we present a cohort of 10 gcGBMs with massive LOH, all of which display near-haploidization, suggesting this event represents a molecular hallmark of a distinct subset of gcGBMs. The identification of this genomic signature provides, for the first time, an ability to link the histomorphology appearance of these tumors with an underlying molecular signature, thus providing the potential for future adoption of an integrated diagnosis. We validated our findings by comparing our cohort against 367 GBMs from the TCGA database. This analysis revealed a distinct copy number landscape in gcGBMs compared to other glioblastomas, with gcGBM demonstrating gains of chromosome 7, as well as frequent gains of chromosomes 1q and 16, but lacking focal aberrations, such as *EGFR* amplification and *CDKN2A* homozygous deletion, which are frequently detected in non-gcGBMs. Importantly, allele-specific copy number analysis identified a pattern of near genome-wide LOH consistent with a near-haploid state. Moreover, performing this analysis on the TCGA GBM dataset led to the identification of 3 additional gcGBMs (3/367), a compelling testament to the observations reported herein. This serendipitous finding resulted solely from comparison of the proportion of the genomes affected by LOH; the histopathologic features of gcGBM were discovered secondarily. Although the presence of undiscovered gcGBMs lacking massive LOH in TCGA remains possible, the previously reported incidences of gcGBM are comparable to what was observed in TCGA, 0.8%.<sup>2-4</sup>

We also characterized the mutational and epigenetic landscape of these tumors. Similar to previously descriptions, gcGBMs demonstrate frequent oncogenic variants in the tumor suppressors *TP53* and *RB1*.<sup>1,5,6</sup> Furthermore, using epigenetic data available for gcGBMs from the TCGA database, we performed methylation analysis, which convincingly differentiated gcGBMs from IDH-mutated GBMs. While gcGBMs largely clustered together, the signature was not sufficiently robust to consistently differentiate these entities from other IDH-wildtype GBMs. Future studies with larger sample size should be dedicated to the methylation signatures of giant cell glial tumors. Overall, these data demonstrate commonality among the gcGBMs that exhibit this massive LOH and may indicate that this signature represents a distinct molecular subtype of these tumors.

Our results substantiate a single case report from nearly 35 years ago which originally describe near-haploidy in a gcGBM<sup>16</sup> and highlights this observation as a reproducible, and likely defining molecular hallmark of a subset of these tumors. Our study thus represents the first allelic-specific copy number analysis of a morphologically homogeneous tumor cohort. We suspect that future studies employing this approach will identify additional gcGBMs with near haploidy. While recent studies highlighted a copy number and mutational profile similar to our cohort, they lacked allelic-specific copy number analyses.<sup>5,6</sup> Our study

highlights the importance of marrying a homogenous histopathology diagnosis with an underlying genomic signature. For example, Cantero et al. investigated tumors with a histopathology diagnosis of gcGBM together with tumors demonstrating a giant cell component.<sup>5</sup> While all tumors in their study shared alterations in *TP53* and some degree of giant cell features, several cases showed additional genetic drivers, such as *IDH1/2* or *BRAF* mutations. As *IDH1/2* mutation status is an important diagnostic marker, which describes both clinical behavior and underlying biology, the inclusion of these tumors in this study highlights the inherent limitation of the current histological criteria. Thus, while p53 deficiency may be an important component driving elements of a giant cell morphology in a subset of tumors, the link between p53 function, near-haploidy, and gcGBM morphology appears much more compelling.

While generally accepted to be a rare mechanism of tumorigenesis, near-haploidy is commonly encountered as a rare but recurrent observation across a wide array of tumors, including inflammatory leiomyosarcoma,<sup>17</sup> oncocytic follicular thyroid carcinoma/Hürthle cell carcinoma,<sup>18,19</sup> adrenocortical carcinoma,<sup>20</sup> and peripheral chondrosarcoma.<sup>21</sup> In these lesions, near-haploidy can be viewed as a defining feature either for the entity or for its clinical behavior. For instance, the genome-wide loss of chromosomes resulting in a near-haploid state correlates with the malignant evolution of osteochondroma to low-grade chondrosarcoma, and subsequent polyploidization or reduplication of those chromosomes marks further transformation to high-grade chondrosarcoma.<sup>21</sup> This series of genomic events is recapitulated in many of the above-mentioned tumor types, serving as a unique mechanism of tumor evolution.<sup>17,18,20,22</sup> The resultant widespread loss of chromosomes has been broadly hypothesized to provide a mechanism whereby many tumor suppressors are lost in one catastrophic event, likely early in tumorigenesis. In support of this hypothesis, a statistically significant association between an increased rate of tumor suppressor mutations and massive LOH has been demonstrated in Hürthle cell carcinoma.<sup>23</sup>

Notably, all gcGBMs evaluated in our study retained heterozygosity of chromosome 7. This pattern was previously demonstrated in the first description of gcGBM with near haploidization and is a commonly reported signature in tumors with massive LOH.<sup>16,19,23</sup> In addition, the ubiquitous preservation of heterozygosity suggests that tumor survival may be dependent on adequate gene dosage. One publication lends support to the hypothesis that imprinted genes necessary for cancer cell survival are present on chromosome 7, necessitating its heterozygosity.<sup>24</sup>

The histopathologic features of our cohort closely mirror those described in previous reports and the WHO classification schema for gcGBM.<sup>1</sup> Nonetheless, several clinicopathologic findings draw inevitable comparison with pleomorphic xanthoastrocytoma (PXA), especially high-grade or “anaplastic” variants. Tumors often occur in a young patient demographic, have a well-circumscribed appearance, and show overlapping microscopic features that include bizarre pleomorphism, reticulin deposition, perivascular lymphocytic inflammation, and occasional eosinophilic granular bodies.



Recent genomic studies, however, demonstrate the nearly universal presence of homozygous *CDKN2A* deletion and mitogen-activated protein kinase (MAPK) activating alterations, most commonly in *BRAF*,<sup>12,25,26</sup> neither of which were observed in any of our gcGBMs. Furthermore, this pattern of near haploidization has not been described in PXA and serves as a useful diagnostic adjunct in cases where this differential diagnosis is being considered, further highlighted by our ability to identify 3 cases of gcGBM from the TCGA GBM cohort by genomic signature alone.

The importance of appropriately defining this entity stems from the need to characterize the clinical significance of this observation. Previous reports suggest that gcGBMs may demonstrate a survival advantage as compared to their non-gcGBM counterparts<sup>2–5,11</sup>; however, the limited follow-up data and recent identification of many of the diagnoses in our cohort precludes definitive assessment of outcomes associated with near haploidization. Nonetheless, it is possible that the frequently well-circumscribed nature of gcGBMs is more amenable to gross total surgical resections and thus improved outcomes. It is also worth noting the prominent inflammatory component in these tumors which may present an attractive target for immunotherapy. While recent phase 3 trials investigating the efficacy of immune therapy in glioblastoma have shown disappointing results,<sup>27</sup> GBM in general is immunologically quiet with minimal lymphocytic infiltrates compared to other tumors that have been successfully treated with immune checkpoint blockade.<sup>28</sup> Similar to inflammatory leiomyosarcomas, it is possible that near haploidization in gcGBM induces a pro-inflammatory state, which in turn may confer improved response to conventional therapies, but further study is clearly needed.

In summary, gcGBM is a rare subtype of IDH-wildtype GBM, currently diagnosed solely on histomorphology. As a group, these tumors are distinguished from their non-gcGBM counterparts by a slightly improved prognosis, decreased overall mutational burden, increased frequency of specific genetic variants, such as *TP53*, and decreased focal copy number changes. These molecular features are not specific enough to confirm the diagnosis for individual cases. We present herein a cohort of gcGBMs with near-haploidy, including massive LOH and retention of chromosome 7 heterozygosity, which when associated with giant cell morphology, represents the genomic hallmark of these entities and aids in their identification for investigative and diagnostic purposes. Future studies with larger cohorts and patient outcome data are necessary to refine molecular criteria required for their more accurate diagnosis, as well as to determine if the subset of gcGBM described herein is distinctive beyond the molecular features, particularly regarding patient outcome and therapeutic response.

## Supplementary Material

Supplementary material is available at *Neuro-Oncology Advances* online.

## Keywords

giant cell glioblastoma | glioblastoma | loss of heterozygosity | near haploidization

## Funding

This work was supported by the Children's Mercy Cancer Center [FP00001036 to L.D.C.].

**Conflict of interest statement.** Y.Y.L. reports equity in g.Root Biomedical Services.

**Authorship Statement:** Data acquisition, writing, formatting, and critical review of the manuscript: T.G.B., J.A., A.M.D., D.J.W., and D.M.M. Neuropathology review: C.T.W., M.G., and D.M.M. Microarray data analysis: I.Z. and L.D.C. Case contribution: L.D.C., M.S.F. and S.S. TCGA data analysis: Y.Y.L. and A.D.C. Acquisition and review of clinical data: S.M.L. Study conception: D.J.W.

## References

1. Louis DN, Ohgaki H, Wiestler OD, et al., eds. *WHO Classification of Tumours of the Central Nervous System*. Revised 4th ed. Lyon, France: International Agency for Research on Cancer; 2016.
2. Kozak KR, Moody JS. Giant cell glioblastoma: a glioblastoma subtype with distinct epidemiology and superior prognosis. *Neuro Oncol*. 2009;11(6):833–841.
3. Ortega A, Nuño M, Walia S, Mukherjee D, Black KL, Patil CG. Treatment and survival of patients harboring histological variants of glioblastoma. *J Clin Neurosci*. 2014;21(10):1709–1713.
4. Jin MC, Wu A, Xiang M, et al. Prognostic factors and treatment patterns in the management of giant cell glioblastoma. *World Neurosurg*. 2019;128:e217–e224.
5. Cantero D, Mollejo M, Sepúlveda JM, et al. TP53, ATRX alterations, and low tumor mutation load feature IDH-wildtype giant cell glioblastoma despite exceptional ultra-mutated tumors. *Neurooncol Adv*. 2020;2(1):vdz059.
6. Shi ZF, Li KK, Kwan JSH, et al. Whole-exome sequencing revealed mutational profiles of giant cell glioblastomas. *Brain Pathol*. 2019;29(6):782–792.
7. Barresi V, Simbolo M, Mafficini A, et al. Ultra-mutation in IDH wild-type glioblastomas of patients younger than 55 years is associated with defective mismatch repair, microsatellite instability, and giant cell enrichment. *Cancers (Basel)*. 2019;11(9):1279.
8. Vande Perre P, Siegfried A, Corsini C, et al. Germline mutation p.N363K in *POLE* is associated with an increased risk of colorectal cancer and giant cell glioblastoma. *Fam Cancer*. 2019;18(2):173–178.

9. Ogawa K, Kurose A, Kamataki A, Asano K, Katayama K, Kurotaki H. Giant cell glioblastoma is a distinctive subtype of glioma characterized by vulnerability to DNA damage. *Brain Tumor Pathol.* 2020;37(1):5–13.
10. Turner R, Matthys S, Heymann J, Gelman B. Imaging findings in the progression of a giant cell glioblastoma. *Radiol Case Rep.* 2018;13(5):1007–1011.
11. Burger PC, Vollmer RT. Histologic factors of prognostic significance in the glioblastoma multiforme. *Cancer.* 1980;46(5):1179–1186.
12. Vaubel RA, Caron AA, Yamada S, et al. Recurrent copy number alterations in low-grade and anaplastic pleomorphic xanthoastrocytoma with and without BRAF V600E mutation. *Brain Pathol.* 2018;28(2):172–182.
13. Garcia EP, Minkovsky A, Jia Y, et al. Validation of OncoPanel: a targeted next-generation sequencing assay for the detection of somatic variants in cancer. *Arch Pathol Lab Med.* 2017;141(6):751–758.
14. Hirschhorn JW, Snider JS, Lindsey KG, Schandl CA. Molecular profiling of vitreous fluid by massively parallel sequencing: a case series. *J Am Soc Cytopathol.* 2020;9(4):254–257.
15. Wang X, Dubuc AM, Ramaswamy V, et al. Medulloblastoma subgroups remain stable across primary and metastatic compartments. *Acta Neuropathol.* 2015;129(3):449–457.
16. Bigner SH, Mark J, Schold SC Jr, Eng LF, Bigner DD. A serially transplantable human giant cell glioblastoma that maintains a near-haploid stem line. *Cancer Genet Cytogenet.* 1985;18(2):141–153.
17. Arbajian E, Köster J, Vult von Steyern F, Mertens F. Inflammatory leiomyosarcoma is a distinct tumor characterized by near-haploidization, few somatic mutations, and a primitive myogenic gene expression signature. *Mod Pathol.* 2018;31(1):93–100.
18. Gopal RK, Kübler K, Calvo SE, et al. Widespread chromosomal losses and mitochondrial DNA alterations as genetic drivers in Hürthle Cell Carcinoma. *Cancer Cell.* 2018;34(2):242–255.e5.
19. Corver WE, Ruano D, Weijers K, et al. Genome haploidisation with chromosome 7 retention in oncocytic follicular thyroid carcinoma. *PLoS One.* 2012;7(6):e38287.
20. Zheng S, Cherniack AD, Dewal N, et al. Comprehensive pan-genomic characterization of adrenocortical carcinoma. *Cancer Cell.* 2016;30(2):363.
21. Bovée JV, van Royen M, Bardoel AF, et al. Near-haploidy and subsequent polyploidization characterize the progression of peripheral chondrosarcoma. *Am J Pathol.* 2000;157(5):1587–1595.
22. Bovée JV, van den Broek LJ, Cleton-Jansen AM, Hogendoorn PC. Up-regulation of PTHrP and Bcl-2 expression characterizes the progression of osteochondroma towards peripheral chondrosarcoma and is a late event in central chondrosarcoma. *Lab Invest.* 2000;80(12):1925–1934.
23. Ganly I, Makarov V, Deraje S, et al. Integrated genomic analysis of Hürthle cell cancer reveals oncogenic drivers, recurrent mitochondrial mutations, and unique chromosomal landscapes. *Cancer Cell.* 2018;34(2):256–270.e5.
24. Boot A, Oosting J, de Miranda NF, et al. Imprinted survival genes preclude loss of heterozygosity of chromosome 7 in cancer cells. *J Pathol.* 2016;240(1):72–83.
25. Vaubel R, Zschoernack V, Tran QT, et al. Biology and grading of pleomorphic xanthoastrocytoma-what have we learned about it? *Brain Pathol.* Published online July 3, 2020. doi:10.1111/bpa.12874.
26. Phillips JJ, Gong H, Chen K, et al. The genetic landscape of anaplastic pleomorphic xanthoastrocytoma. *Brain Pathol.* 2019;29(1):85–96.
27. McGranahan T, Therkelsen KE, Ahmad S, Nagpal S. Current state of immunotherapy for treatment of glioblastoma. *Curr Treat Options Oncol.* 2019;20(3):24.
28. Thorsson V, Gibbs DL, Brown SD, et al. The immune landscape of cancer. *Immunity.* 2018;48(4):812–830.e14.